

# MR-based Bony 3D models enable radiation-free preoperative patient-specific analysis and 3D printing for SCFE patients

Till D Lerch<sup>1,2</sup>, Tilman Kaim<sup>1,3</sup>, Valentin Grob<sup>1</sup>, Markus Hanke<sup>4</sup>, Florian Schmaranzer<sup>1</sup>, Simon D Steppacher<sup>4</sup>, Jasmin D Busch<sup>1</sup>, and Kai Ziebarth<sup>5</sup>

## Abstract

**Objectives:** Slipped capital femoral epiphyses (SCFE) is a common pediatric hip disease with the risk of osteoarthritis and impingement deformities, and 3D models could be useful for patient-specific analysis. Therefore, magnetic resonance imaging (MRI) bone segmentation and feasibility of 3D printing and of 3D ROM simulation using MRI-based 3D models were investigated.

**Methods:** A retrospective study involving 22 symptomatic patients (22 hips) with SCFE was performed. All patients underwent preoperative hip MR with pelvic coronal high-resolution images (T1 images). Slice thickness was 0.8–1.2 mm. Mean age was  $12 \pm 2$  years (59% male patients). All patients underwent surgical treatment. Semi-automatic MRI-based bone segmentation with manual corrections and 3D printing of plastic 3D models was performed. Virtual 3D models were tested for computer-assisted 3D ROM simulation of patients with knee images and were compared to asymptomatic contralateral hips with unilateral SCFE (15 hips, control group).

**Results:** MRI-based bone segmentation was feasible (all patients, 100%, in 4.5 h, mean  $272 \pm 52$  min). Three-dimensional printing of plastic 3D models was feasible (all patients, 100%) and was considered helpful for deformity analysis by the treating surgeons for severe and moderate SCFE. Three-dimensional ROM simulation showed significantly ( $p < 0.001$ ) decreased flexion ( $48 \pm 40^\circ$ ) and IR in  $90^\circ$  of flexion ( $-14 \pm 21^\circ$ , IRF- $90^\circ$ ) for severe SCFE patients with MRI compared to control group ( $122 \pm 9^\circ$  and  $36 \pm 11^\circ$ ). Slip angle improved significantly ( $p < 0.001$ ) from preoperative  $54 \pm 15^\circ$  to postoperative  $4 \pm 2^\circ$ .

**Conclusion:** MRI-based 3D models were feasible for SCFE patients. Three-dimensional models could be useful for severe SCFE patients for preoperative 3D printing and deformity analysis and for ROM simulation. This could aid for patient-specific diagnosis, treatment decisions, and preoperative planning. MRI-based 3D models are radiation-free and could be used instead of CT-based 3D models in the future.

**Keywords:** Slipped capital femoral epiphysis, 3D model, 3D printing, in situ pinning

<sup>1</sup>Department of Diagnostic, Interventional and Paediatric Radiology, Inselspital, University of Bern, Bern, Switzerland

<sup>2</sup>Department of Orthopaedic Surgery, Child and Young Adult Hip Preservation Program at Boston Children's Hospital, Harvard Medical School, Boston, MA, USA

<sup>3</sup>Graduate School for Health Sciences, University of Bern, Switzerland

<sup>4</sup>Department of Orthopedic Surgery, Inselspital, University of Bern, Bern, Switzerland

<sup>5</sup>Department of Pediatric Surgery, section of pediatric orthopedic surgery, Inselspital, University of Bern, Bern, Switzerland

Date received: 14 March 2023; accepted: 12 January 2024

## Corresponding Author:

Till D Lerch, Department of Radiology, Inselspital Bern, Freiburgstrasse, 3010 Bern, Switzerland.

Emails: till.lerch@insel.ch; till.lerch@childrens.harvard.edu



## Introduction

Slipped capital femoral epiphysis (SCFE) is a common hip disorder in adolescents. SCFE is a well-recognized hip disease that can lead to disability, femoroacetabular impingement (FAI), and osteoarthritis.<sup>1,2</sup> Several femoral osteotomies have been described to correct the deformity, such as the Imhauser osteotomy<sup>3</sup> (flexion osteotomy), basicervical closing wedge femoral neck osteotomy<sup>4</sup> (according to Dunn), or triplane proximal femoral osteotomy<sup>5</sup> or the modified Dunn procedure. In case of severe SCFE, a modified Dunn procedure<sup>6,7</sup> may be performed to improve hip mechanics.<sup>6</sup> Independent of the type of osteotomy used, deformity correction (especially in severe chronic SCFE) can be complex due to the three-dimensional (3D) deformity.<sup>8</sup> Usually, 2D radiographs are used for diagnosis. But, radiographs are influenced by patient positioning.<sup>9</sup>

Recently, advances in magnetic resonance imaging (MRI) techniques and the increasing availability of additive manufacturing methods (3D printing) enabled clinical use. One of the clinical applications is surgical planning for orthopedic procedures. A previous study used patient-specific CT-based 3D printed models for surgical planning<sup>5</sup> for SCFE patients. CT-based 3D models of the bone were previously used for pediatric deformities,<sup>10</sup> pelvic osteotomies,<sup>11,12</sup> spine surgery,<sup>13</sup> and orthopedic trauma surgery.<sup>14</sup> But due to the radiation dose of CT scans,<sup>15</sup> CT-based osseous 3D models have not been applied to clinical routine so far in our institution. The use of CT scans has increased tremendously in the last two decades.<sup>16</sup> Using high-resolution MRI images for routine preoperative MRI, we aimed for 3D printed MRI-based osseous 3D models. MRI-based 3D printed models would enable radiation-free analysis, surgical planning, and for treatment decision of open hip preservation surgery (e.g., femoral osteotomy or the modified Dunn procedure). Feasibility of plastic 3D-printed models based on MRI was tested. Therefore, (1) MRI bone segmentation and (2) feasibility of 3D printing and (3) 3D ROM simulation using MRI 3D models were investigated.

## Methods

A retrospective study involving 22 symptomatic patients (22 hips) with SCFE was performed. Mean age was  $12 \pm 2$  years (59% male, Table 1). Institutional Review Board approval was obtained prior to this study. All patients were from a single institution (Inselspital Bern, University Hospital Bern, Switzerland). Inclusion criteria for this study were the following: all patients required a diagnosis of a symptomatic SCFE, a preoperative MRI scan of the pelvis and surgical treatment. This resulted in 30 SCFE patients between 09/2016 and 01/2021. Of 30 SCFE patients, 5 patients had MRI in an external institution in this time period, 2 patients had no high-resolution images, and 1 was

**Table 1.** Demographic information of the patient series is shown.

Parameter	Value
Total hips (patients)	22 (22)
Age at operation (year)	12 (10–15)
Gender (% male of all hips)	59
Unstable hips according to Loder et al. <sup>17</sup> classification	6 hips
Severity based on slip angle <sup>18</sup>	
Mild <30°	7 hips
Moderate 30°–60°	7 hips
Severe >60°	8 hips
Classification based on the duration of symptoms	
Acute	2 hips
Acute on chronic	9 hips
Chronic	11 hips
Postoperative slip angle (°)	4 (2–10)

a syndromal patient. The remaining 22 SCFE patients underwent MRI with high-resolution images in our institution and were used for bone segmentation.

Mean preoperative slip angle was  $47^\circ \pm 20^\circ$  (range 25°–70°), while eight patients had a severe slip and seven patients had a moderate slip (Table 1), and seven hips had a mild slip. Moderate SCFE was defined by a slip angle of between 30° to 60°, also called epiphyseal-shaft angle, while severe SCFE was defined as >60°. Most patients (16 patients) presented with a stable SCFE and six hips with an unstable slip, according to Loder et al.<sup>17</sup> classification. Acute on chronic slips were noted in 9 patients, chronic in 11 patients, and acute SCFE in 2 patients (Table 1).

## MR imaging

All patients underwent preoperative pelvic radiographs (ap and lateral) and MR imaging of the hip joint and the pelvis. Preoperative hip MRI was performed on 3Tesla (8 patients) or 1.5Tesla scanner (Siemens Medical Solutions, Erlangen, Germany) with large flexible surface coils and multiplanar T1-weighted images in coronal, and PD-weighted images in sagittal, axial, and coronal orientation. High-resolution images (coronal pelvic T1 StarVIBE flash 3D images on 3Tesla and T1 VIBE on 1.5 Tesla) were used for diagnostic purposes and for bone segmentation (VIBE=Volume interpolated breath-hold examination). The field of view (FOV) of the bilateral high-resolution images covered the entire pelvis from the anterior superior iliac spine to the level below the lesser trochanter (Figure 1(a)). Slice thickness for T1 StarVIBE was 1.2mm, and the voxel size was  $1.2 \times 1.0625 \times 1.0625$  mm for high-resolution images (Supplemental Table S1). For the T1 VIBE, the voxel size was  $0.8 \times 0.78125 \times 0.78125$  mm. Detailed parameters of the high-resolution images are provided in Supplemental Table S1. Scan time for high-resolution images was 3 min and 39 s (T1 StarVIBE) and 5 min and 11 s (T1 VIBE).

Overall scan time of the MRI examination was 30–40 min. In addition to the routine protocol, a bilateral 3D sequence of the knee joint (T1 VIBE Dixon) was used for eight severe SCFE patients for ROM simulation. Unfortunately, five of the 22 patients had no available images of the knee joints. Three patients underwent additional 3D sequence of the pelvis (T1 VIBE Dixon).

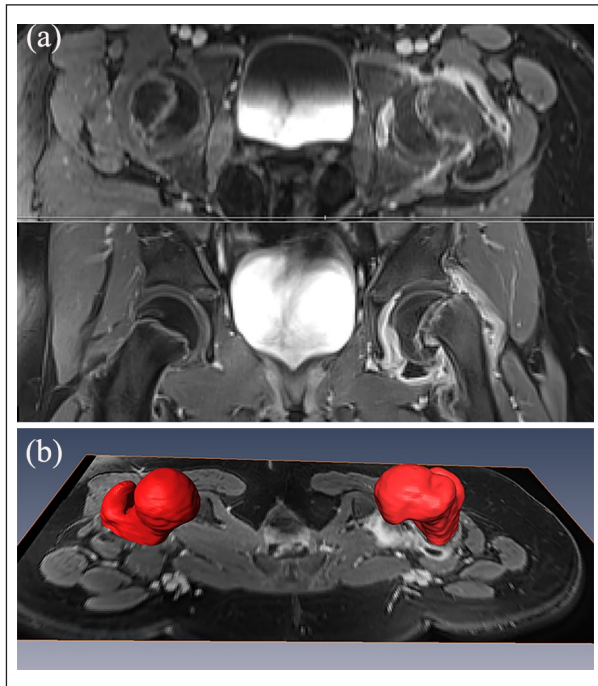


**Figure 1.** Preoperative transverse (axial, top) and coronal (below) T1-weighted MR images (StarVIBE) of a female patient with SCFE are shown. Three-dimensional models (red) of the SCFE side and of the contralateral side are shown (b). MR: magnetic resonance; SCFE: slipped capital femoral epiphyses.

## Image processing

Image processing of the high-resolution MR images (Figure 1(a)) was performed in a semi-automatic fashion using the commercial software AMIRA Visualization Toolkit (Visage Imaging Inc, Carlsbad, CA, USA). Bone segmentation of MR-based osseous 3D models of the acetabulum and proximal femur was performed separately (Figure 1(b)). This resulted in virtual 3D models of the hip joints of all SCFE patients (Figure 2). High-resolution MR images with a maximal 1.2 mm slice thickness were used for bone segmentation of 3D models (Figure 1(a) and (b)). High-resolution MR images were processed by segmentation, smoothing, and conversion to stereolithography (STL) 3D printable format (Video 1) by one observer with 5 years of experience in musculoskeletal radiology. For the knee joint, the segmentation was performed separately on axial T1 VIBE Dixon images with 1 mm slice thickness using the same software. For the control group, asymptomatic contralateral hips with unilateral SCFE (15 hips) and preoperative 3D-CT were used. The control group was available from a previous study (Lerch, Kim and Kiapour, 2022).

## Three-dimensional model printing

Virtual 3D models were converted to STL files (Video 1). The STL files were checked for irregularities or for noise speckles, which were removed. STL files were then optimized for 3D printing using an automated mesh repair function. Used software for slicing was UP Studio (Tiertime Corporation). Each resulting STL file was printed with Polylactic Acid on a 3D printer Cetus 3D MK1 (Manufacturer Wuxi Tiertime Technology Co., Ltd.). The cost for this 3D printer was 349 USD. The used 3D printer had a three-axis module, a printing build volume of

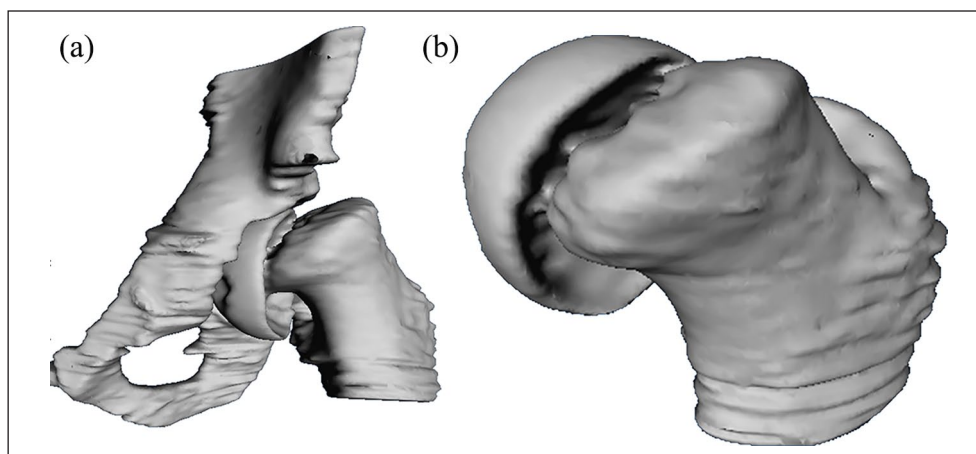


**Figure 2.** Virtual 3D models of a male SCFE patient of the hip joint (a) and of the proximal femur (b) are shown based on bone segmentation using high-resolution MR images. MR: magnetic resonance; SCFE: slipped capital femoral epiphyses.

180 × 180 × 180 mm, and a total weight of 3.2 kg. Plastic 3D models were printed with melted extrusion modeling without a fill pattern with automatically generated supports. A pilot study was performed to select the most appropriate filling pattern and printing parameters for plastic 3D models.

### Three-dimensional ROM simulation

The virtual 3D models were loaded in software for dynamic 3D ROM simulation (Figure 3). The specific software uses a validated collision detection algorithm<sup>19</sup> to assess virtual hip ROM (Table 2). Flexion, internal and external rotation in 90° of flexion, was calculated with 1° steps (Video 2). Furthermore, combined motion patterns (Video 2) can be analyzed, such as Drehmann's sign or the widely used anterior impingement test, also called the Flexion-Adduction-internal rotation (FADIR) test.<sup>20</sup> Location of impingement (Video 2 and 3) can be visualized for acetabulum and femur separately.<sup>21,22</sup> The software was described in detail in Table 2 and in previous publications.<sup>22,23</sup>

### Surgical treatment

The included 22 SCFE patients underwent surgical treatment: 15 hips underwent the modified Dunn procedure, while two hips underwent surgical hip dislocation for cam resection. Five hips with mild SCFE underwent in situ pinning. The indication for the modified Dunn procedure was hip pain and a positive Drehmann's sign<sup>24</sup> with moderate to severe deformity at the proximal head-neck junction as defined by a slip angle of more than 30°. The operative technique of the modified Dunn procedure has been previously described in detail.<sup>25</sup> The indication for surgical treatment was not influenced by 3D printed models. Three-dimensional printed models were performed retrospectively after the surgical decision making.

### Statistical analysis

Statistical analysis was performed using Winstat software (R. Fitch Software, Bad Krozingen, Germany). Normal distribution was tested using the Kolmogorov-Smirnov test for continuous variables. Radiographic measurements of the slip angle were independently performed by one observer not involved in surgical care of the patients. The slip angle (continuous variable) was compared using the Wilcoxon test because the data was not normally distributed.

### Results

1. MRI-based 3D segmentation (Figure 1(b)) was feasible in all patients (100%, duration of 4.5 h, mean  $272 \pm 52$  min). The segmentation had a duration of more than 5 h for five patients. Bone

segmentation was more time-consuming for the T1 VIBE images (1.5 Tesla) compared to the StarVIBE images (3 Tesla).

2. Three-dimensional printing of the 3D models (Figure 4) was feasible in all patients (100%). All 3D printed models of moderate and severe SCFE patients were considered helpful for deformity analysis by the treating surgeons. Some 3D-printed models were used for the explanation of the deformity to the patients.
3. Dynamic 3D ROM simulation (Figure 3) was feasible in eight severe SCFE patients with MRI images of the pelvis and knee and enabled visualization of femoral and acetabular impingement locations. Three-dimensional ROM simulation showed significantly ( $p < 0.001$ ) decreased flexion ( $48 \pm 40^\circ$ ) and IR in 90° of flexion ( $-14 \pm 21^\circ$ , IRF-90°) for severe SCFE patients compared to control group ( $122 \pm 9^\circ$  and  $36 \pm 11^\circ$ ). For one patient with severe SCFE, preoperative impingement-free flexion was limited to 40° and to 60° (for another patient) due to impaction-type impingement of the metaphysis on the superior acetabular rim (Video 2 and 3). The mean slip angle improved significantly ( $p < 0.001$ ) from preoperative  $54 \pm 15^\circ$  (40–70) to postoperative of  $4 \pm 2^\circ$  (2–10).

### Discussion

A retrospective study with 22 SCFE patients investigating feasibility of MRI-based 3D printed models was performed. Three-dimensional printing and ROM simulation were feasible with virtual MRI-based 3D models of preoperative high-resolution MR images. The 3D ROM simulation was investigated in eight severe SCFE patients.

MRI-based segmentation of 3D models and printing of plastic 3D models were feasible in this study. It was evaluated to see if this would be helpful for deformity analysis. In addition, these MRI-based 3D models of severe SCFE patients were used for patient-specific 3D ROM simulation. Given the radiation of pelvic CT and fluoroscopy,<sup>15</sup> decreased radiation exposure with this young patient group of childbearing age may be beneficial. One of the potential advantages of the 3D model was that the treating surgeon could gain a 3D understanding of the individual and patient-specific proximal femoral deformity and the direction of slippage. Theoretically, it is possible to simulate hip surgery using the printed plastic 3D models to plan the amount of correction that would need to be performed to optimize hip range of motion (e.g., optimal femoral osteotomy or cam resection to avoid subsequent FAI).

This is one of few studies that used radiation-free MRI images for 3D printing of patient-specific 3D models (Figure 4). Another strength of this study is that this method allows the visualization of hip impingement

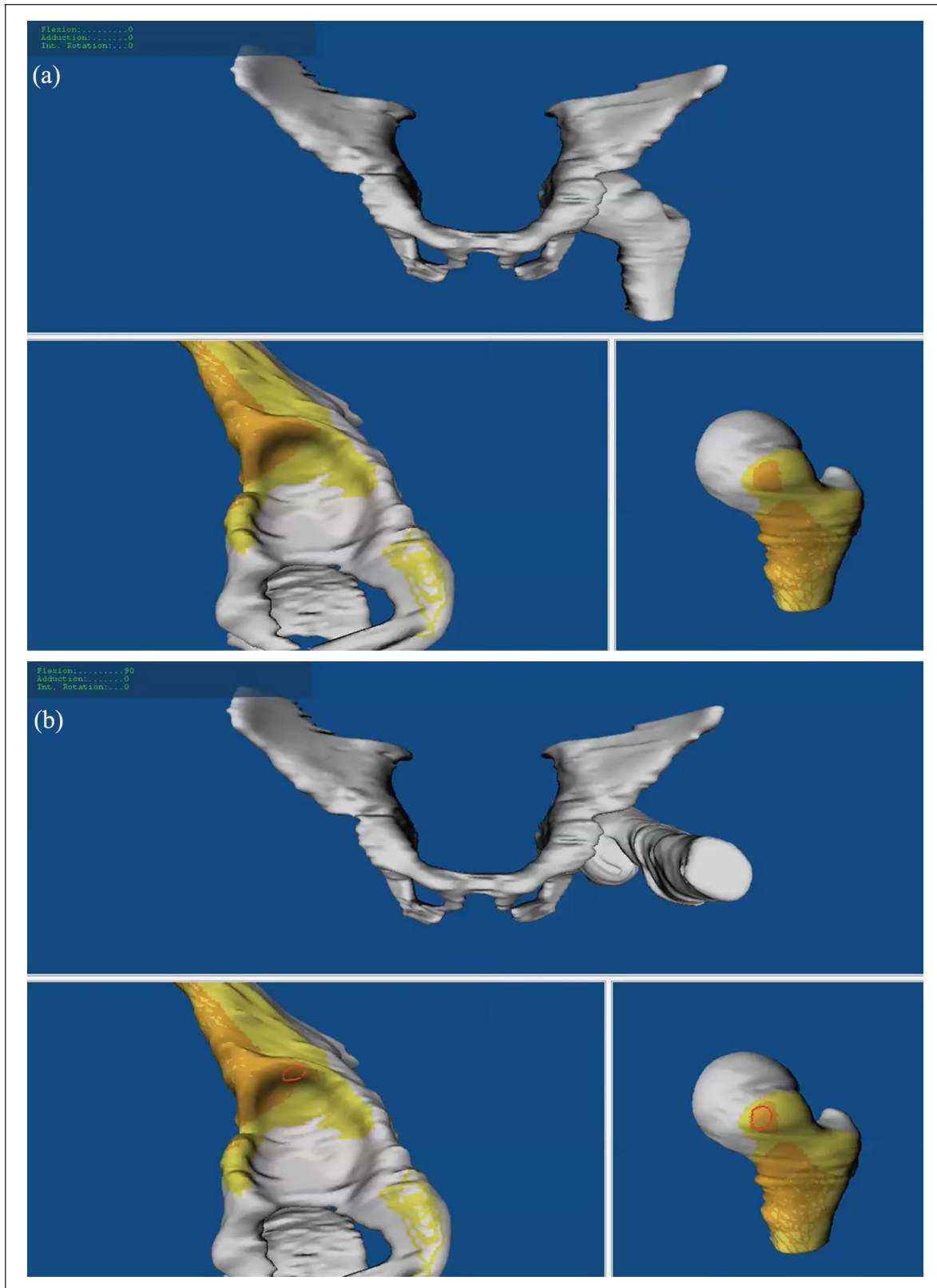


**Figure 3.** Impingement simulation without impingement (a) and with impingement (b, red area) in 90° of flexion is shown for a patient with severe SCFE. The location of impingement is shown with the red area (b) on the superior acetabulum and on the anterior metaphysis using 3D impingement simulation and MRI-based 3D models.

**Table 2.** Details of the collision detection software using patient-specific osseous 3D models of the hip joint.

Software tool	Description/definition
Anterior pelvic plane (APP) was used as acetabular reference coordinate system	Defined by landmarks of both anterosuperior iliac spines and the pubic tubercles.
Femoral reference coordinate system	Defined by landmarks of the femoral head center, the knee center, and both femoral condyles.
Automatic rim detection	For automatic detection of the osseous acetabular rim.
Best-fitting sphere algorithm	For identification of the femoral head center.
Equidistant method	For virtual impingement-free hip motion analysis.
Distribution of the impingement zones	Was calculated using a previously described clock face system.
Clockface coordinate system	Three o'clock was defined anteriorly for both right and left hips. The 6 o'clock represents the acetabular notch.
Intra-articular impingement	Intra-articular locations included the acetabular rim on the acetabular side and the femoral head and neck on the femoral side.

APP: anterior pelvic plane.



**Figure 4.** Two 3D printed plastic models of the proximal of a patient with severe SCFE (right) and moderate SCFE (left) are shown.

SCFE: slipped capital femoral epiphyses.

(Figure 3). For evaluation of anterior FAI, flexion and internal rotation in 90° of flexion<sup>21</sup> were used for simulation of the anterior impingement test (also called FADIR test). Detailed 3D information about the size and shape of the lunate surface is important for the decision making for surgical therapy in patients with FAI.<sup>26</sup>

A novel finding is that segmentation of MRI-based 3D models was possible with routine MRI images. Former investigations for MRI-based 3D models of the hip joint and femur used different MRI protocols (not during clinical routine application) and different methods to generate the 3D models.<sup>27,28</sup> Various reasons including long acquisition time, small FOV, inhomogeneous bone intensity, or unclear boundaries between bone and the soft tissue could explain that. To the best of the author's knowledge, no other study investigating the feasibility of MRI-based 3D

models for SCFE patients was found in the literature. Previous studies compared the bone segmentation results or the CT-based or MRI-based generation of 3D models in cadavers<sup>29,30</sup> or with different patients or methods for bone segmentation.<sup>23</sup>

This study has several important clinical implications. Surgical treatment of SCFE was limited by surgeon's inability to preoperatively assess the exact location of hip impingement. Impingement location was observed intraoperatively. But, preoperative radiation-free methods for planning and executing any femoral osteotomy are lacking for SCFE patients.<sup>5</sup> To address this problem, MRI-based 3D models using software for collision detection were evaluated. But, due to the radiation dose of CT scans,<sup>15</sup> this software has not been applied to clinical routine for SCFE patients in our institution. The routine use of CT scans seems not suitable for adolescents or young patients of childbearing age. Previous studies used CT scans for 3D modeling for SCFE patients.<sup>5,31,32</sup> This CT method allows detailed simulation of hip preservation surgery (such as osteochondroplasty or femoral osteotomy) for SCFE patients<sup>31,32</sup> of childbearing age. For severe SCFE patients, different types of femoral osteotomies can be simulated while the effect of cam resection (osteochondroplasty) on hip range of motion can be simulated for mild SCFE patients.<sup>32</sup> CT scans with dose reduction or low dose protocol could be used, but this decreases the bone-soft tissue contrast, and this makes it difficult for bone segmentation. Routine clinical application of MR-based 3D models can potentially reduce the need for preoperative CT scans in young and active patients of childbearing age with hip pain due to SCFE. Furthermore, MR-based 3D models could allow the future application of ROM simulation in children with other hip deformities such as FAI and hip dysplasia. In addition, cartilage and labrum damage could be evaluated using MRI, and this could help for preoperative planning if open intra-articular hip surgery is needed.

For FAI patients, 3D-printed models are an important tool to treat complex or combined hip deformities and improve surgical outcomes.<sup>33–36</sup> Full-sized 3D models of the proximal femur allow for better understanding of the direction of slippage and visualization of the unique 3D deformity of SCFE and therefore improve preoperative planning, which resulted in shorter surgery time, less fluoroscopy exposure, and lower complication rate.<sup>5</sup>

Preoperative planning is crucial when performing corrections of complex 3D deformities. Traditionally, orthopedic procedures were planned using radiographs or 2D CT scans and other methods to determine optimal bone alignment. This is especially challenging in patients with SCFE because the deformity of the femoral epiphysis shows malalignment in all three dimensions (coronal, sagittal, and axial). In addition, the severity of deformity in each plane varies between patients and can cause FAI. Three-dimensional printing of 3D models provides a unique opportunity to better understand the deformity and to determine the patient-specific correction needed to optimize hip biomechanics. In addition, these 3D models were printed at relatively low costs (350 dollars for the 3D printer used for this study). However, this is not a low-cost method, considering the costs for MRI scan (estimated 500–600 dollars, depending on scan time and other factors) and the estimated costs for up to 4–5 h of image processing. This method may not be applicable to low-income countries.

The study had a number of limitations. The study group has limited power because a small patient sample size was reviewed retrospectively. This was primarily due to the low incidence of moderate to severe stable SCFE at a single institution. In the current study, 3D modeling of the osseous pelvis and the proximal femur was used for each patient, without taking into account soft tissue (labrum, muscles, or cartilage). This is a well-known limitation for computer simulation of hip ROM.<sup>21</sup> Due to image artifacts during the acquisition of MRI in patients with previous operations and screw fixation, patients with previous operations were not evaluated in the current study. This limits the applicability of this method to patients without implants, which could be the case, for example, after previous in situ pinning. MRI examinations are expensive and have limited availability, this limits applicability worldwide. In addition, manual corrections and steps were performed during the bone segmentation of the 3D models. Manual correction of bone segmentation and manual localization of osseous landmarks are examples of performed manual steps. These manual steps are potential sources of error and interobserver variability and are time-consuming. Future studies could investigate automatic and less time-consuming methods for bone segmentation. In addition, we could not demonstrate improved treatment decision making or patient-specific preoperative planning in the current study. However, previous studies demonstrated the usefulness of CT-based 3D models for 3D modeling<sup>31,32</sup> and for 3D printing<sup>5</sup> for severe

SCFE patients. Therefore, it can be assumed that MR-based 3D models could be as helpful as CT-based 3D models for these patients, although not directly investigated in this study.

## Conclusion

MRI-based 3D models of the hip for SCFE patients were feasible for 3D printing. Three-dimensional models can be useful for severe SCFE patients for 3D printing and for ROM simulation. This could aid for patient-specific preoperative planning and could help with deformity analysis. Three-dimensionally printed MRI-based models are radiation-free and could be used instead of CT-based 3D models for the simulation of open hip preservation surgery such as femoral osteotomy.

## Author contributions

**Till D Lerch:** Conceptualization, data curation, formal analysis, investigation, methodology, project administration, visualization, writing—original draft, writing—review and editing, drafting the article or revising it critically for important intellectual content, final approval of the version to be submitted.

**Tilman Kaim:** Data curation, formal analysis, final approval of the version to be submitted.

**Valentin Grob:** Data curation, formal analysis, 3D printing.

**Markus S Hanke:** Data curation, formal analysis, final approval of the version to be submitted.

**Florian Schmaranzer:** Conceptualization, supervision, validation drafting the article, or revising it critically for important intellectual content, final approval of the version to be submitted.

**Simon D Steppacher:** Conceptualization, supervision, validation.

**Jasmin D Busch:** Conceptualization, supervision, validation.

**Kai Ziebarth:** Conceptualization, supervision, validation.

## Declaration of conflicting interests

The author(s) declared no potential conflicts of interest with respect to the research, authorship, and/or publication of this article.

## Funding

The author(s) disclosed receipt of the following financial support for the research, authorship, and/or publication of this article: Till Lerch has received funding for this study of the Swiss National Science Foundation, Early Postdoc. Mobility Grant Number P2BEP3\_195241. The authors thank the Swiss National Science Foundation.

## Ethical approval

Each author certifies that his or her institution approved the human protocol for this investigation, that all investigations were conducted in conformity with ethical principles of research, and that informed consent for participation in the study was obtained.

## ORCID iDs

Till D Lerch  <https://orcid.org/0000-0002-0475-0269>

Florian Schmaranzer  <https://orcid.org/0000-0002-8729-7243>

## Supplemental material

Supplemental material for this article is available online.

## References

- Carney BT, Weinstein SL and Noble J. Long-term follow-up of slipped capital femoral epiphysis. *J Bone Joint Surg Am* 1991; 73: 667–674.
- Leunig M, Casillas MM, Hamlet M, et al. Slipped capital femoral epiphysis: early mechanical damage to the acetabular cartilage by a prominent femoral metaphysis. *Acta Orthop Scand* 2000; 71(4): 370–375.
- Baraka MM, Hefny HM, Thakeb MF, et al. Combined Imhauser osteotomy and osteochondroplasty in slipped capital femoral epiphysis through surgical hip dislocation approach. *J Child Orthop* 2020; 14: 190–200.
- DeRosa GP, Mullins RC and Kling TF Jr. Cuneiform osteotomy of the femoral neck in severe slipped capital femoral epiphysis. *Clin Orthop Relat Res* 1996; 322: 48–60.
- Cherkasskiy L, Caffrey JP, Szewczyk AF, et al. Patient-specific 3D models aid planning for triplane proximal femoral osteotomy in slipped capital femoral epiphysis. *J Child Orthop* 2017; 11(2): 147–153.
- Ziebarth K, Milosevic M, Lerch TD, et al. High survivorship and little osteoarthritis at 10-year followup in SCFE patients treated with a modified dunn procedure. *Clin Orthop Relat Res* 2017; 475(4): 1212–1228.
- Lerch TD, Vuilleumier S, Schmaranzer F, et al. Patients with severe slipped capital femoral epiphysis treated by the modified Dunn procedure have low rates of avascular necrosis, good outcomes, and little osteoarthritis at long-term follow-up. *Bone Joint J* 2019; 101-B(4): 403–414.
- Paez CJ, Bomar JD, Farnsworth CL, et al. Three-dimensional analysis of acetabular morphology and orientation in patients with slipped capital femoral epiphysis. *J Pediatr Orthop* 2021; 41: e130–e134.
- Jones CE, Cooper AP, Doucette J, et al. Southwick angle measurements and SCFE slip severity classifications are affected by frog-lateral positioning. *Skeletal Radiol* 2018; 47: 79–84.
- Facco G, Massetti D, Coppa V, et al. The use of 3D printed models for the pre-operative planning of surgical correction of pediatric hip deformities: a case series and concise review of the literature. *Acta Biomed* 2022; 92: e2021221.
- Caffrey JP, Jeffords ME, Farnsworth CL, et al. Comparison of 3 pediatric pelvic osteotomies for acetabular dysplasia using patient-specific 3D-printed models. *J Pediatr Orthop* 2019; 39(3): e159–e164.
- Shelton TJ, Monazzam S, Calafi A, et al. Preoperative 3D modeling and printing for guiding periacetabular osteotomy. *J Pediatr Orthop* 2021; 41: 149–158.
- Al-Khouja L, Shweikeh F, Pashman R, et al. Economics of image guidance and navigation in spine surgery. *Surg Neurol Int* 2015; 6(suppl. 10): S323–S326.
- Li K, Liu Z, Li X, et al. 3D printing-assisted surgery for proximal humerus fractures: a systematic review and meta-analysis. *Eur J Trauma Emerg Surg* 2022; 48(5): 3493–3503.
- Wylie JD, Jenkins PA, Beckmann JT, et al. Computed tomography scans in patients with young adult hip pain carry a lifetime risk of malignancy. *Arthroscopy* 2018; 34(1): 155.e3–163.e3.
- Hall EJ and Brenner DJ. Cancer risks from diagnostic radiology. *Br J Radiol* 2008; 81: 362–378.
- Loder RT, Richards BS, Shapiro PS, et al. Acute slipped capital femoral epiphysis: the importance of physeal stability. *J Bone Joint Surg Am* 1993; 75(8): 1134–1140.
- Southwick WO. Osteotomy through the lesser trochanter for slipped capital femoral epiphysis. *J Bone Joint Surg Am* 1967; 49(5): 807–835.
- Puls M, Ecker TM, Tannast M, et al. The Equidistant Method—a novel hip joint simulation algorithm for detection of femoroacetabular impingement. *Comput Aided Surg* 2010; 15(4–6): 75–82.
- Casartelli NC, Brunner R, Maffiuletti NA, et al. The FADIR test accuracy for screening cam and pincer morphology in youth ice hockey players. *J Sci Med Sport* 2018; 21: 134–138.
- Lerch TD, Siegfried M, Schmaranzer F, et al. Location of intra- and extra-articular hip impingement is different in patients with pincer-type and mixed-type femoroacetabular impingement due to acetabular retroversion or protrusio acetabuli on 3D CT-based impingement simulation. *Am J Sports Med* 2020; 48(3): 661–672.
- Tannast M, Kubiak-Langer M, Langlotz F, et al. Noninvasive three-dimensional assessment of femoroacetabular impingement. *J Orthop Res* 2007; 25(1): 122–131.
- Zeng G, Degonda C, Boschung A, et al. Three-dimensional magnetic resonance imaging bone models of the hip joint using deep learning: dynamic simulation of hip impingement for diagnosis of intra- and extra-articular hip impingement. *Orthop J Sports Med*. Epub ahead of print 24 November 2021. DOI: 10.1177/23259671211046916.
- Kamegaya M, Saisu T, Nakamura J, et al. Drehmann sign and femoro-acetabular impingement in SCFE. *J Pediatr Orthop* 2011; 31(8): 853–857.
- Tannast M, Jost LM, Lerch TD, et al. The modified Dunn procedure for slipped capital femoral epiphysis: the Bernese experience. *J Child Orthop* 2017; 11(2): 138–146.
- Steppacher SD, Lerch TD, Gharanzadeh K, et al. Size and shape of the lunate surface in different types of pincer impingement: theoretical implications for surgical therapy. *Osteoarthr Cartilage* 2014; 22(7): 951–958.
- Gilles B and Magnenat-Thalmann N. Musculoskeletal MRI segmentation using multi-resolution simplex meshes with medial representations. *Med Image Anal* 2010; 14(3): 291–302.
- Morbée L, Vereecke E, Laloo F, et al. MR Imaging of the Pelvic Bones: The Current and Cutting-Edge Techniques. *J Belg Soc Radiol* 2022; 106(1):123. <https://pubmed.ncbi.nlm.nih.gov/36475022/>
- Florkow MC, Willemsen K, Mascarenhas VV, et al. Magnetic Resonance Imaging Versus Computed Tomography for Three-Dimensional Bone Imaging of Musculoskeletal Pathologies: A Review. *J Magn Reson Imaging*. 2022; 56(1):11–34. <https://pubmed.ncbi.nlm.nih.gov/35044717/>



30. Van den Broeck J, Vereecke E, Wirix-Speetjens R, et al. Segmentation accuracy of long bones. *Med Eng Phys* 2014; 36(7): 949–953.
31. Lerch TD, Kim Y-J, Kiapour AM, et al. Limited hip flexion and internal rotation resulting from early hip impingement conflict on anterior metaphysis of patients with untreated severe SCFE using 3D modelling. *J Pediatr Orthop* 2022; 42: e963–e970.
32. Lerch TD, Kim Y-J, Kiapour A, et al. Do osteochondroplasty alone, intertrochanteric derotation osteotomy, and flexion-derotation osteotomy improve hip flexion and internal rotation to normal range in hips with severe SCFE? A 3D-CT simulation study. *J Pediatr Orthop* 2023; 43: 286–293.
33. Schmaranzer F, Helfenstein R, Zeng G, et al. Automatic MRI-based Three-dimensional Models of Hip Cartilage Provide Improved Morphologic and Biochemical Analysis. *Clin Orthop Relat Res.* 2019; 477(5):1036-1052. <https://pubmed.ncbi.nlm.nih.gov/30998632/>.
34. Verma T, Mishra A, Agarwal G, et al. Application of three dimensional printing in surgery for cam type of femoro-acetabular impingement. *J Clin Orthop Trauma* 2018; 9(3): 241–246.
35. Wong TT, Lynch TS, Popkin CA, et al. Preoperative use of a 3D printed model for femoroacetabular impingement surgery and its effect on planned osteoplasty. *AJR Am J Roentgenol* 2018; 211(2): W116–W121.
36. Zeng G, Degonda C, Boschung A, et al. Three-Dimensional Magnetic Resonance Imaging Bone Models of the Hip Joint Using Deep Learning: Dynamic Simulation of Hip Impingement for Diagnosis of Intra- and Extra-articular Hip Impingement. *Orthop J Sports Med* 2021; 9(12):23259671211046916. <https://pubmed.ncbi.nlm.nih.gov/34938819/>